First results on radiometric dating of metals by alpha spectrometry ☆

J. Cruz [a,b,*], E. Figueiredo [c], V. Corregidor [d], P.I. Girginova [b], L.C. Alves [e], C. Cruz [d], R.J.C. Silva [c], I. Liritzis [f]

[a] LIBPhys-UNL, DF, FCT, Universidade NOVA de Lisboa, 2829-516 Monte de Caparica, Portugal
[b] Centro de Física Nuclear da Universidade de Lisboa, Av. Prof. Gama Pinto, 1649-003 Lisboa, Portugal
[c] CENIMAT/I3N, DCM, FCT, Universidade NOVA de Lisboa, 2829-516 Monte de Caparica, Portugal
[d] IPFN, IST-UL, Campus Tecnológico e Nuclear, E.N. 10, 2695-066 Sacavém, Portugal
[e] C2TN, IST-UL, Campus Tecnológico e Nuclear, E.N. 10, 2695-066 Sacavém, Portugal
[f] King Saud University, Kingdom of Saudi Arabia, and, Laboratory of Archaeometry, Dept of Mediterranean Studies, University of the Aegean, 1 Demokratias Ave., Rhodes 85100, Greece

ARTICLE INFO

ABSTRACT

A new TSAC (Thick Source Alpha Particle Counting spectrometry) setup of high geometrical efficiency and low intrinsic background was built to measure the alpha particles coming from the ^{238}U and ^{232}Th decay chains radionuclides with concentrations down to the ppm level. It was designed to test the ^{226}Ra/^{230}Th method, which is the only direct metal dating method proposed to date. Micro-PIXE, micro-RBS and SEM-EDS were used as complementary analytical techniques in order to search for heterogeneities and/or impurities that could bias the TSAC data. Ores, resulting slags and metallic prills from two recent smelting experiments that reproduced ancient techniques and two ancient coins were studied to determine how radionuclides fractionation occurs during smelting. With this TSAC setup the background signal was extremely low, but comparable to the signal from the measured metals. Preliminary results show no evidence of a preferential depletion of ^{226}Ra in a melted metal with respect to the other radionuclides.

1. Introduction

Archaeometallurgical research focuses in the reconstruction of early trade routes in terms of location of metal sources (ore deposits) and in the study of metallic artifacts and metallurgical remains through various analytical and examination techniques. Important information can be derived from these studies, like ore provenance, contact between different ancient societies and their technological development.

It's not an overstatement to say that the Holy Grail of archaeometallurgists is to achieve a method that can directly give the date of the manufacture of a metallic artifact.

Until now, the dating of metallurgical processes is made indirectly, under favorable conditions, by [1]: a) thermoluminescence (TL) and optical stimulated luminescence (OSL) of burnt soil in kilns and crucibles, or of remaining core material in the metal artifact and slag products [2]; b) radiocarbon (^{14}C) applied on carbon found in trapped slag inclusions (mainly iron artifacts); c) association with other archeological artifacts found in the same archeological context; and d) some aging or degradation specificities that may differentiate an old from a new object (e.g. intergranular corrosion is a slower corrosion process).

In 2006 [1] I. Liritzis proposed a radiometric dating method for metals that are produced from ores (native metals excluded), based on the isotopic fractionation that may occur during ore smelting. This fractionation disrupts the secular equilibrium in the ^{238}U series. In this sense, ^{226}Ra, a radionuclide that occurs naturally in the decay chain of ^{238}U with a half-life of 1602 years, tends to be withdrawn by slag products away of the melted metal, as a result of its low specific gravity, 5–6 g/cm^3, and its lower melting point (700 °C) when compared to some metals, as for example copper (8.9 g/cm^3; 1083 °C).

As a consequence, in a metal, ^{226}Ra would appear from the decay of its parent, ^{230}Th (half-life, $t_{1/2} = 80000$ years). Assuming that initially in the metal ^{226}Ra is not present, then at time t, the ratio between the activities of ^{226}Ra and ^{230}Th is given by Eq. (1) [1]

$$\frac{A_{226Ra}}{A_{230Th}} = \frac{\lambda_{226Ra}}{\lambda_{226Ra} - \lambda_{230Th}} \left[1 - e^{-(\lambda_{226Ra} - \lambda_{230Th})t} \right], \qquad (1)$$

where λ_{226Ra} and λ_{230Th} are the decay constants ($\lambda = \ln(2)/t_{1/2}$) of ^{226}Ra and ^{230}Th, respectively. As $\lambda_{226Ra} >> \lambda_{230Th}$ (4.33×10^{-4} yr^{-1} $>> 8.66 \times 10^{-6}$ yr^{-1}) the ratio of activities tend to the value $\lambda_{226Ra} / (\lambda_{226Ra} - \lambda_{230Th}) \approx 1$, and the secular equilibrium is attained after around 9000 years. This period is comparable to the elapsed time since the onset of metallurgy in some areas of the globe. Therefore, this growth of ^{226}Ra back to secular equilibrium with its parent ^{230}Th is the basis of this method. This model, known as the ^{226}Ra/^{230}Th Liritzis method,

can be considered theoretically consistent. However, its experimental validation still needs to be done. The key issues for this validation are:

- very low counting rate: ores contain traces of uranium (^{238}U and ^{235}U, with natural abundances of 99.284% and 0.72%, respectively), thorium (^{232}Th, with 100% natural abundance) and their daughter products derived from their radioactive decay. ^{232}Th series is taken into account in this study because it interferes with the measurements of ^{226}Ra and ^{230}Th. On average, uranium in copper ores is 2.4 ppm (1–3 ppm) and thorium is 0–1 ppm [1,3]. These concentration values are very low, so in order to get statistically relevant data, a high efficiency measurement system must be used together with a strict control and minimization of background sources;
- the efficient separation/fractionation of U and Th daughter products during smelting lacks in literature. In the geological field, primitive lavas present high ^{226}Ra/^{238}U ratios that can be explained in a scenario of selective fractionation [1], but in the field of metallurgy, the fractioning efficiency is poorly understood because it depends on a variety of mechanisms operating in a smelting furnace, such as: a) sorting by density, b) sorting by melting point, c) sorting by chemical affinity (with strong influence on the thermodynamic conditions in the furnace) and d) differences in solubilities [4].
- radionuclide homogeneity in ores, metals and slags. In principle, it is expected homogeneity in ores since the uranium and thorium series are in equilibrium. For the metals and slags produced after ore smelting, it is expected that if there is no secular equilibrium a heterogeneous distribution of radionuclides can be present at a microstructural level, due to normal microstructural heterogeneities of the produced materials (as production of different phases in some alloys and the development of various mineralogical compounds in slags). However, this non-homogeneity is mostly expected at the microstructural level; the analysis of "macro-areas" should yield an average value.

According to Eq. (1), the ^{226}Ra/^{230}Th (Liritzis) method implies the quantification of both radionuclides present in a sample. Considering that ^{226}Ra and its progenitor, ^{230}Th, decay by emitting alpha particles – ^{226}Ra emits alpha particles with energies 4.784 MeV (94.45%) and 4.601 MeV (5.55%), while the alpha particles from the ^{230}Th have energies of 4.687 MeV (76.3%) and 4.620 MeV (23.4%) – the TSAC (Thick Source Alpha Particle Counting spectrometry [5,6]) is a suitable technique to detect the presence of these radionuclides. Furthermore, the TSAC technique is accurate, sensitive to all alpha emitters from the uranium and thorium series, 15 in total (8 from the ^{238}U series and 7 from the ^{232}Th series), non-destructive (a fundamental point in the study of any rare and valuable metallic artifact), well suited to handle samples of several centimeters in size and masses of several grams, and it is a setup simple and easily portable to museum installations. The only constrain factors are that it is a technique sensitive to approximately only the first 10–20 μm of the sample, which is the range of alpha particles with energies between 4 and 8 MeV in a metal (thus can be considered as a superficial analysis); and the data acquisition period can be considered relatively long (several days are needed). Additionally, as the analyzed samples are thick, the alpha particles emitted in depth loose energy before they reach the sample surface producing a continuum energy distribution in a TSAC spectrum. This results in a more complex spectrum to analyze. However it will allow determining whether there is secular equilibrium or not and eventually where this disequilibrium occurs.

In this work the used experimental setup is described and preliminary results are presented and discussed, constituting the first step in testing the ^{226}Ra/^{230}Th dating method, which may provide a secure basis for the application and development of the unique metal dating method proposed to date, and as such it will be especially important with respect to artifacts that have been found out of datable archaeological contexts, or where archaeological contexts have been lost, or even to detect forgeries.

2. Material and methods

2.1. Studied objects

The methodology followed in this work rests on measuring the TSAC spectra for two sets of samples:

1. copper and tin ores, resulting slags and metallic prills from two recent smelting experiments: a) smelting tin ores (cassiterite — SnO$_2$) by traditional and simple means (an ethnoarchaeographic approach); b) smelting tin (cassiterite) and copper ores (malachite — Cu$_2$CO$_3$(OH)$_2$) for the production of bronze, simulating ancient smelting techniques, namely those performed in open air fires (in crucibles) which have been used since Chalcolithic times to Iron Age in various regions of Europe. With the complete chain of materials involved in the smelting available, it is possible to study how radionuclide separation occurs during smelting. Here, the key issue is how efficient is the removal of ^{226}Ra to the slags: once metal is separated from slag, ideally ^{226}Ra will be associated with slag and metal will be free of radium. However, in practice traces may remain. If this happens the age obtained by the ^{226}Ra/^{230}Th method will be higher than the real one, and the discrepancy increases with the amount of radium that remained in the metal;
2. coins from different centuries. The option for the study of coins comes from the fact that coins cover a wide period of metallurgy, their age is well known, they are made of different metals or alloys, they have similar shapes (which simplifies the experimental setup) and, frequently they are well preserved (absence or low level of surface corrosion). In this case, it must be considered the possibility of metal recycling, since it is well known that coins, as well as other metallic artifacts, were often obtained by re-melting previous objects. When metal is re-melted to make a new object, the equilibrium is disrupted because radon and polonium are removed, though soon after some days, equilibrium is set again; thus, the ^{226}Ra and ^{230}Th activities and their activity ratio are not affected by re-melting process. Consequently, in the case of measuring the age of a coin made by recycled metal the age refers to the smelting process and not to the later re-melting, meaning that the age obtained by the ^{226}Ra/^{230}Th method will give an older date than the date of the object fabrication. The study of different coins from different epochs will allow verification of this. In this work, the results for two Portuguese coins are presented, a bullion coin named "dinheiro" from king Fernando I (ruler of Portugal between 1367 and 1383), and a "III Réis" copper coin minted in 1874 (under the reign of king Luís I).

All samples were cleaned with alcohol in an ultrasonic cleaning bath before the measurements and their surface was optically inspected with an Olympus SZX9 stereo microscope searching for some noticeable surface deposits.

2.2. Thick Source Alpha Particle Counting spectrometry (TSAC)

The alpha detector selected for this work is a specially designed PIPS detector (model A1200-32AM) from Canberra Industries (Meriden, U.S.A.) with a large surface area (1200 mm^2), energy resolution of 32 keV (FWHM) and a very low intrinsic background (nominal value below 0.67 counts/h in the energy range of 3 to 8 MeV) [7]. The pulses produced by the detector were processed and shaped by an ORTEC142 (not cooled) preamplifier and an ORTEC571 amplifier from ORTEC (Oak Ridge, U.S.A.) which are then digitized by a MCA-8000D Multichannel Analyzer from Amptek Inc. (Bedford, U.S.A.) to give a 4096 channels alpha particle energy spectrum up to ~10 MeV (2.5 keV/channel). In order to increase the number of counts per channel, the spectra were compressed to 1024 channels. Because of that the quantization error increased as we went from a 2.5 keV/channel to a 10 keV/channel configuration; nevertheless it is still suitable for this work.
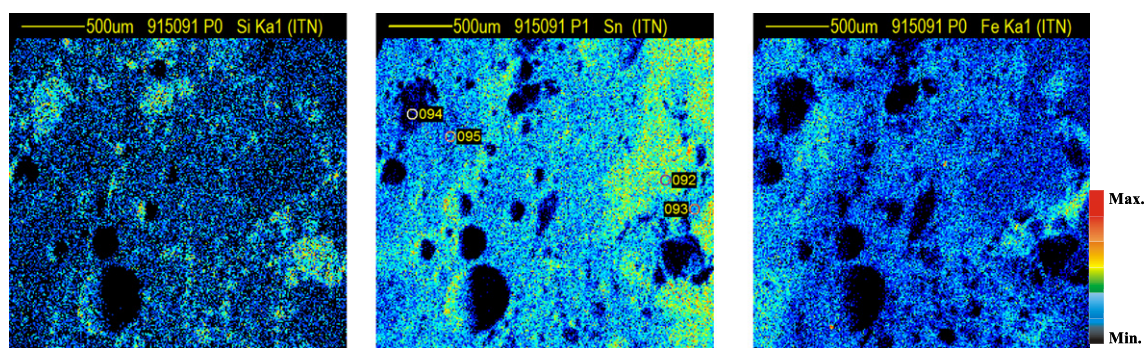
Fig. 1. Slag sample 2D PIXE surface maps (scan 2640x2640 μm²) for Si, Sn and Fe obtained with a 2 MeV proton beam. The numbered circles in the Sn map indicate the location of point analysis (3 × 4 μm²).

Alpha particles spectra were taken in vacuum conditions ($P \approx 5 \times 10^{-6}$ mbar) with the PIPS detector mounted on top of a PVC sample holder (distance sample-detector ≈ 5 mm, meaning a geometric efficiency of approximately 0.334 for a sample with a diameter of 32 mm). The TSAC setup was operated in a temperature controlled room, contributing to the electronic chain stability. This stability was checked by the regular use of a pulse generator together with a triple alpha (^{244}Cm, ^{241}Am, ^{240}Pu) calibration source.

The quoted uncertainties for TSAC arise from the uncertainty in number of counts, N, recorded in the energy range of 3 to 8 MeV. The results are presented in terms of activity (counts per hour), with a corresponding statistical uncertainty given by the maximum (δ_i, δ_e), with

$$\delta_i = \left[\sum_{j=1}^{n} \frac{1}{\delta y_j^2}\right]^{-1/2}, \quad \delta_e = \left[\frac{\sum_{j=1}^{n}\left(\overline{y}-y_j\right)^2 \frac{1}{\delta y_j^2}}{(n-1)\sum_{j=1}^{n}\frac{1}{\delta y_j^2}}\right]^{1/2},$$

where the variable y stands for $N/\Delta t$ (Δt is the duration of each of the n runs performed for each sample).

2.3. Microstructural and elemental analyses by μ-PIXE, μ-RBS and SEM-EDS

To complement TSAC measurements, μ-PIXE (micro-Particle Induced X-ray Emission), μ-RBS (micro-Rutherford Backscattering Spectrometry) and SEM-EDS (Scanning Electron Microscopy with Energy Dispersive Spectroscopy) were used in order to determine elemental distribution and composition of the objects while searching for particular surface heterogeneities and/or impurities that could bias the results of TSAC.

Combined μ-PIXE and μ-RBS analyses were performed using proton beams of 1 or 2 MeV produced by the 2.5 MV Van de Graaff Accelerator of the CTN/IST (Lisbon, Portugal). An Oxford Microbeams type nuclear microprobe was used (OM150 triplet system), which allowed the proton beam to be focused on the samples with a spatial resolution of 3×4 μm² under vacuum conditions. With this set-up it is also possible to perform beam scans over the surface of the samples up to 2640×2640 μm² when using 2 MeV proton beams [8] to obtain 2D elemental distribution maps. To detect the X-rays, a 30 mm² SDD X-ray detector with a 145 eV energy resolution, positioned at 135° to the beam direction, was used. To filter the low energy X-ray signal and prevent protons entering the X-ray detector when working with 2 MeV proton beam, a 50 μm foil of Mylar is used. The backscattered protons are collected by a PIPS detector in Cornell geometry at 140° to the beam direction.

The OMDAQ V5.2 software package [9] is used for data acquisition and treatment. This software also allows us to control the beam by the scanning control. Spectra evaluation and quantification was done with the GUPIX [10] code for PIXE spectra while RBS spectra were fitted with the NDF code [11]. It should be remarked that these techniques are also superficial, and that with a 2.0 MeV proton beam, PIXE can analyze the same depth region as TSAC.

SEM examinations were conducted in a Zeiss DSM 962 equipment (Zeiss Group, Oberkochen, Germany), with a secondary electrons
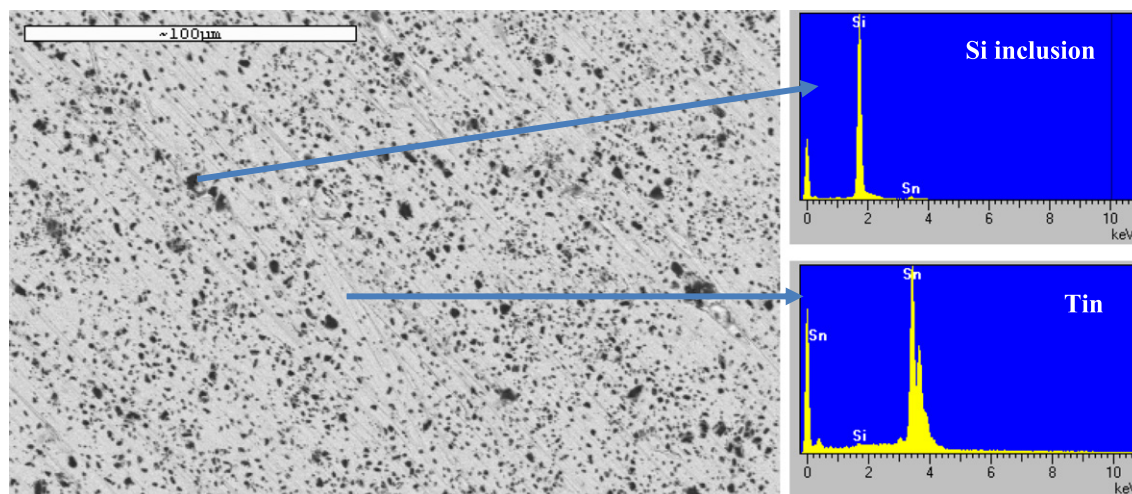

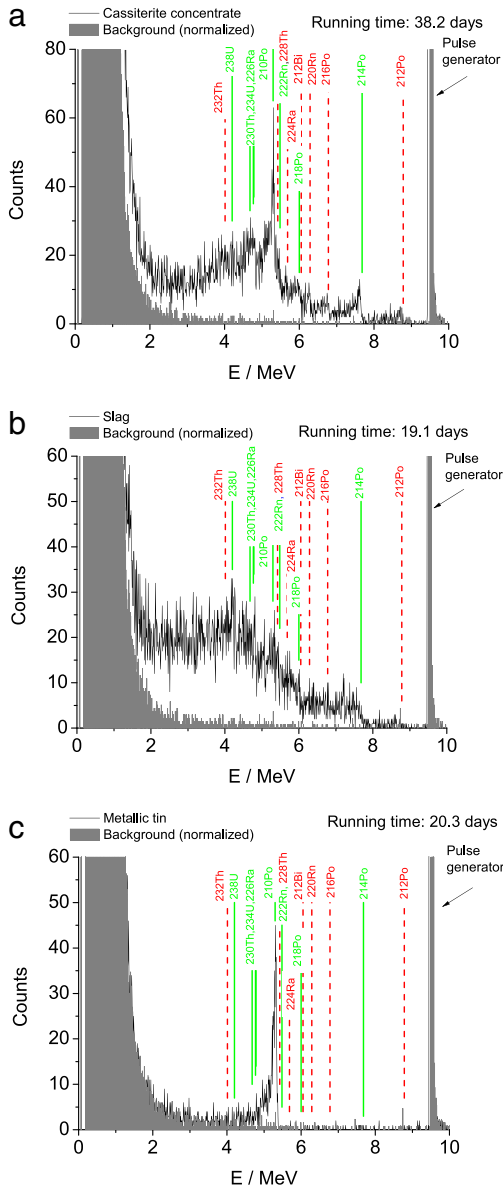**Fig. 2.** SEM-EDS (BSE image mode) for metallic tin, showing various Si inclusions.

Fig. 3. TSAC spectra from tin smelting experiment. (a) Cassiterite concentrate; (b) slag; (c) metallic tin. Solid lines: energies from the ^{238}U series isotopes. Dashed lines: energies from the ^{232}Th series isotopes. Background signal (shadow).
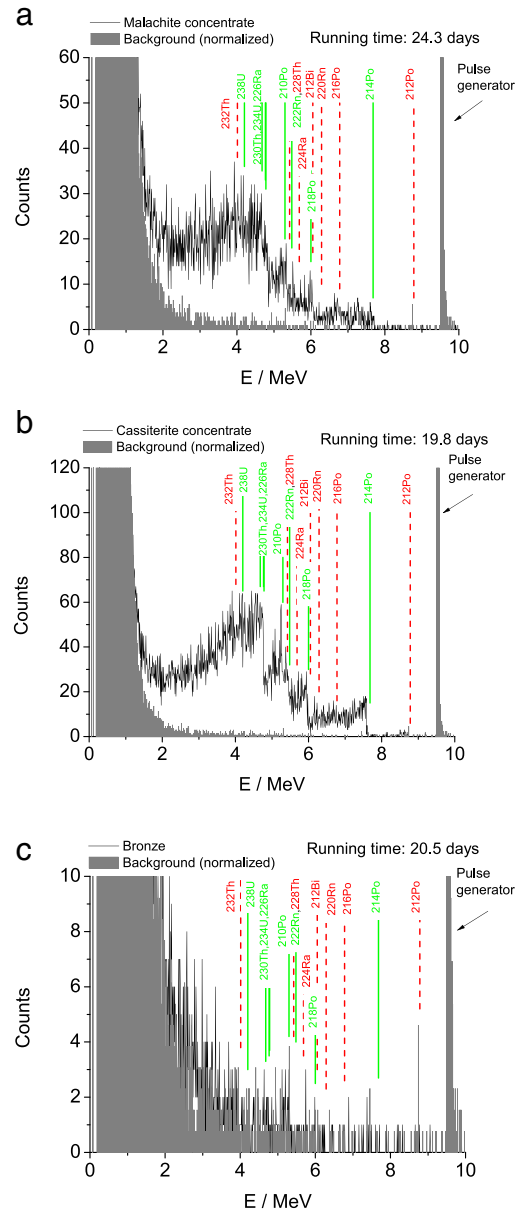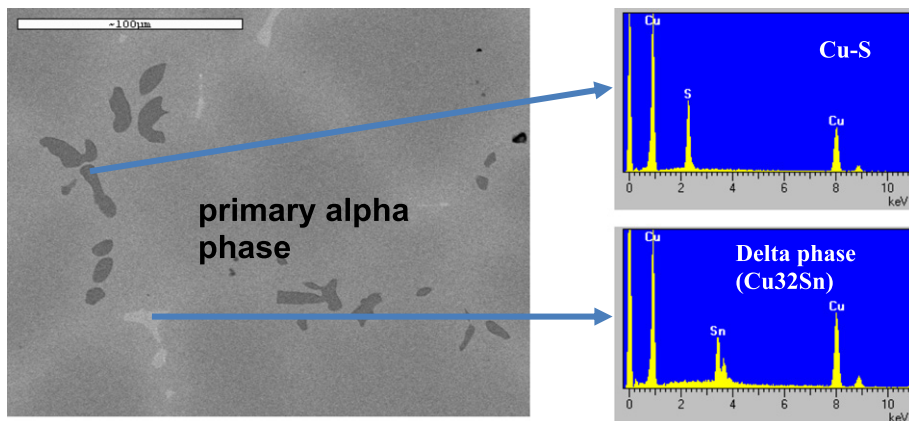
Fig. 5. TSAC spectra from bronze smelting experiment. (a) Malachite concentrate; (b) cassiterite concentrate; (c) metallic bronze. Solid lines: energies from the ^{238}U series isotopes. Dashed lines: energies from the ^{232}Th series isotopes. Background signal (shadow).

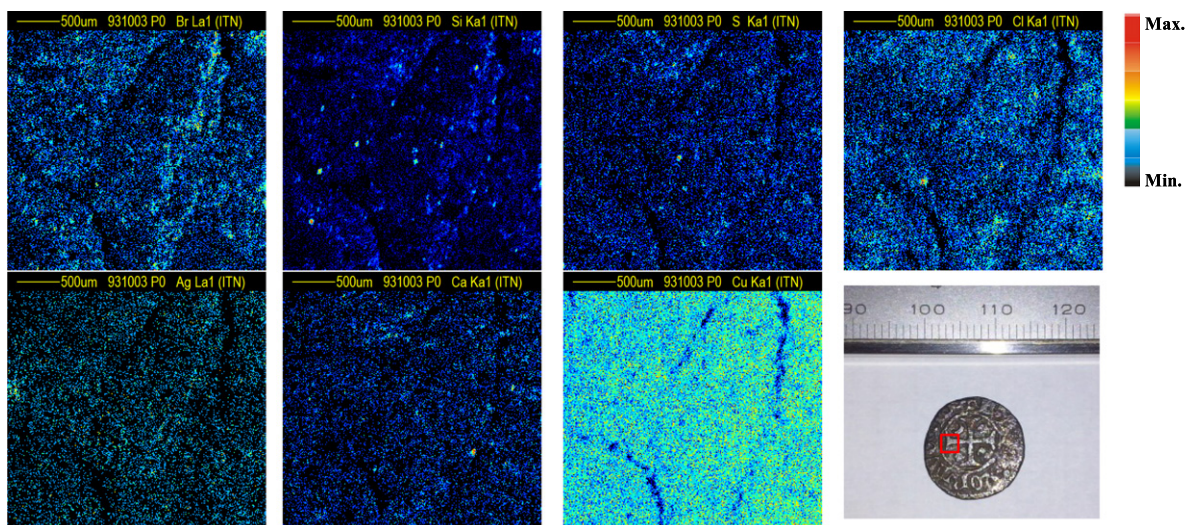**Fig. 4.** SEM-EDS (BSE image mode) for metallic bronze with ~8 wt.% Sn.

Fig. 6. "Dinheiro" 2D PIXE surface maps (scan 2980 × 2980 µm^2) for Br, Si, S, Cl, Ag, Ca and Cu obtained with a 1 MeV proton beam. The open square drawn on the coin indicates the analyzed coin surface.

detector (SE), backscattered electrons detector (BSE) and an energy dispersive spectrometer (EDS) from Oxford Instruments INCAx-sight (Oxford Instruments, Abingdon, United Kingdom) with an ultra-thin window that enables the detection of oxygen and carbon. Semi-quantifications were made using ZAF correction procedure. Experimental conditions were 20 kV of voltage, approximately 3 A of filament current, 25 mm of work distance and 70 µA of emission current. The samples were polished in the examined region, and a gold coating was used for slags, while for metals only a carbon tape bridge from the polished area to the ground was applied.

3. Results and discussion

3.1. TSAC background

In order to register the background signal during the TSAC experiments, the first measurements performed had no sample inside the PVC holder. For a total running time of 26.3 days (35 runs), a yield of 277 counts was obtained in the energy range of 3–8 MeV, which means 0.44 ± 0.03 counts/h, 34% lower than the nominal value given by Canberra (0.67 counts/h). The background spectrum results from: a) electronic noise (low energy); b) beta particles (E ≤ 2.25 MeV) and alpha particles (E ≤ 8.78 MeV) emissions from the ^{238}U and ^{232}Th series located in the PVC holder and in the detector itself; and c) cosmic rays (essentially muons) that cross Earth's atmosphere and deposit some energy in the PIPS detector. This background will be presented superimposed in the spectra obtained for each studied sample and normalized in time.

3.2. Smelting experiments

3.2.1. Tin smelting products

The microstructural and elemental analyses performed on the cassiterite concentrate and the resulting slags reveal a heterogeneous elemental surface distribution with high concentrations of Sn and Si (in the form of oxides), as exemplified in Fig. 1 that shows the 2D maps (2640 × 2640 µm^2) obtained by µ-PIXE with a 2 MeV proton beam for a slag sample. In the Sn map, the numbered circles indicate the point analysis locations (3 × 4 µm^2) which allowed quantification of elemental concentration variations (pre-established oxides): SnO$_2$ 0.23–50.7 wt.%, SiO$_2$ 38.6–99.4 wt.%, CaO 0.00–6.57 wt.%, TiO$_2$ 0.04–3.83 wt.%, MnO 0.01–6.43 wt.%, and Fe$_2$O$_3$ 0.14–19.1 wt.%.

Identical analyses performed on the metallic tin show a homogeneous distribution composed essentially of metallic tin with Si inclusions, with the superficial distribution presented in the SEM-EDS image of Fig. 2.

Considering the sensitivity of these techniques (µg/g for combined µ-PIXE and µ-RBS and mg/g for SEM-EDS), these results show that these samples can be analyzed by TSAC since the heterogeneities and impurities detected do not seem able to bias the TSAC results.

Fig. 3 shows the TSAC spectra obtained for the cassiterite concentrate, the resulting slags and the metallic tin superimposed on the normalized background spectrum. The cassiterite concentrate was measured for 38.2 days (33 runs) with a yield of 6106 counts in the energy range of 3–8 MeV, or 6.68 ± 0.09 counts/h, a value 15.2 times higher than the background yield above mentioned of 0.44 ± 0.03 counts/h. The slags were measured for 19.1 days (15 runs) with a yield of 6257 counts in the energy range of 3–8 MeV, or 13.7 ± 0.3 counts/h, a value 31.1 times higher than the background yield. The
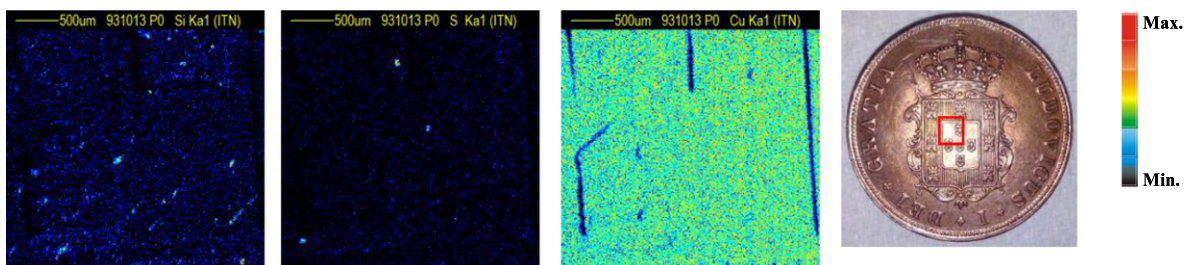

Fig. 7. "III Réis" 2D PIXE surface maps (scan 2980 × 2980 µm^2) for Si, S and Cu obtained with a 1 MeV proton beam. The open square drawn on the coin indicates the analyzed coin surface.

metallic tin was measured for 20.3 days (14 runs) with a yield of 1057 counts in the energy range of 3–8 MeV, or 2.18 ± 0.07 counts/h, a value 5.0 times higher than the background yield. However, more than half of these counts, 570, form a surface peak at the ^{210}Po energy (5.3043 MeV). In the cassiterite concentrate spectrum, an identical peak is also present alongside with a small peak at the ^{214}Po energy (7.6868 MeV). These structures indicate an excess of these isotopes on the samples surface and most likely result from some type of contamination. The number of detected alpha particles, N_α, depends on the number of ^{210}Po and ^{214}Po atoms present in the sample at the beginning of the measurement, N_0, according to the radioactive decay law: $N_\alpha = N_0 - N_0 \exp(-\lambda t)$. For the ^{210}Po ($t_{1/2} = 138.376$ days), $N_\alpha = 570$ were detected in $t = 20.3$ days, giving $N_0 \approx 6000$ in the metallic tin; for the cassiterite concentrate, $N_\alpha = 330$ and $t = 38.2$ days, giving $N_0 \approx 1900$ atoms. These values are extremely low when compared with typical atomic densities in solids which are around 10^{23} atoms/cm^3, and far below the detection limits of PIXE, RBS and SEM-EDS. The observed ^{210}Po excess may result from external sources, for instance atmospheric pollutants coming from the tobacco smoke or fertilizers. It has been reported that tobacco leaves used in making cigarettes contain radioactive material, particularly ^{210}Pb (decays by beta emission) and ^{210}Po. The radionuclide content of tobacco leaves depends heavily on soil conditions and fertilizer use, namely phosphate fertilizers [12]. For the ^{214}Po ($t_{1/2} = 0.1636$ ms), $N_\alpha \approx 70$ were detected in $t = 38.2$ days, giving $N_0 \approx 70$ in the cassiterite concentrate, a negligible value.

The different alpha particle yields measured for the ore, the slags and the metal show that no significant signals were detected in the metal, while in the ore and slags it is possible to detect alpha particle emissions at the characteristic energies.
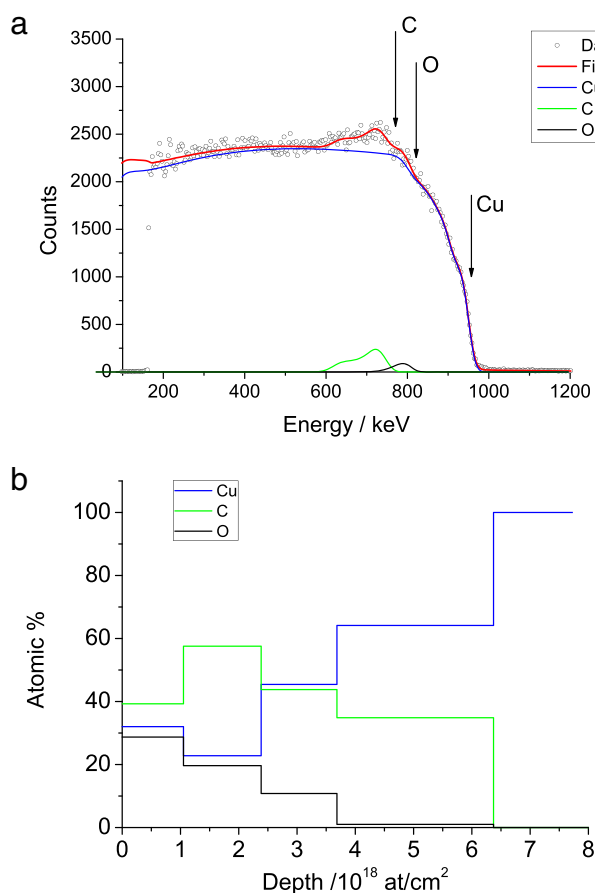
3.2.2. Bronze smelting products

The microstructural and elemental analyses performed on the cassiterite and malachite concentrates, resulting slags and bronze prills that resulted from the smelting experience didn't show any heterogeneities or impurities that could bias the TSAC measurements.

In Fig. 4, results of the microstructural examination by SEM-EDS of one bronze prill with Sn ≈ 8 wt.% show the formation of delta eutectoid and Cu–S inclusions.

Fig. 5 shows the TSAC spectra obtained for the malachite and cassiterite concentrates, and for the bronze prills (slag spectra are still not available). The malachite concentrate was measured for 24.3 days (33 runs) with a yield of 5627 counts in the energy range of 3–8 MeV, or 9.7 ± 0.2 counts/h, a value 22 times higher than the background yield. The cassiterite concentrate was measured for 19.8 days (17 runs) with a yield of 12395 counts in the energy range of 3–8 MeV, or 26.1 ± 0.3 counts/h, a value 59 times higher than the background yield. In this spectrum a peak at the ^{210}Po energy is also visible. As for the bronze, it was measured for 30.9 days (21 runs) with a yield of 452 counts in the energy range of 3–8 MeV, or, 0.62 ± 0.05 counts/h, a value 1.4 times higher than the background yield.

These yields show that, as in the tin case, no significant signals were detected in the metal, while in the starting ores it is possible to detect alpha particle emissions at the characteristic energies.

3.3. Copper coins

The elemental analysis performed with μ-PIXE and μ-RBS on the two studied copper-based coins also didn't show any heterogeneities or impurities that could bias the TSAC measurements. The 2D maps (2980×2980 μm^2) obtained by μ-PIXE using a proton beam of 1 MeV for the "dinheiro" (Fig. 6) and for the "III Réis" (Fig. 7) show that the surfaces have only a few scattered inclusions containing Br, Si, S, Cl and Ca which are typical corrosion products. The presence of superficial C and
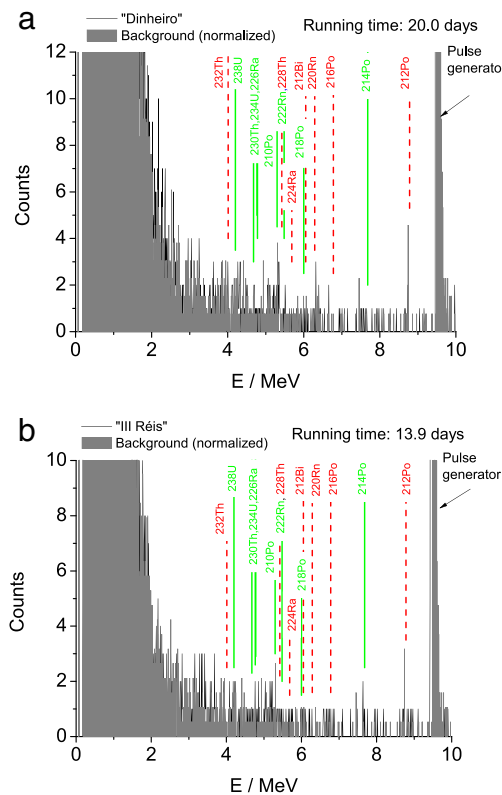

Fig. 8. (a) μ-RBS spectrum fitted with NDF. (b) Elemental depth profile for Cu, C and O (6×10^{18} at/cm^2 ≈ 0.7 μm). Coin: "dinheiro".

Fig. 9. TSAC spectra for the "dinheiro" (a) and for the "III Réis" (b) coins. Solid lines: energies from the ^{238}U series isotopes. Dashed lines: energies from the ^{232}Th series isotopes. Background signal (shadow).

O was signaled by μ-RBS as exemplified in Fig. 8a. The presence of these two elements extends down to ≈ 0.7 μm in depth (Fig. 8b).

Fig. 9 shows the TSAC spectra obtained for the "dinheiro" and the "III Réis". For the first coin, a total running time of 20.0 days (14 runs) yielded 245 counts in the energy range of 3–8 MeV, or 0.51 ± 0.04 counts/h, a value 16% higher than the background yield. For the "III Réis" coin, a total running time of 13.9 days (8 runs) yielded 171 counts in the energy range of 3–8 MeV, or 0.51 ± 0.04 counts/h, the same as obtained for the "dinheiro". In line with the results obtained for the metallic tin and the metallic bronze no significant signals were detected for these two coins.

4. Final remarks

The TSAC setup built to test the ^{226}Ra/^{230}Th method reached an extremely small background yield (0.44 ± 0.03 counts/h in the energy range of 3 to 8 MeV). This value is smaller than the yield obtained for the metal samples. However, the difference is still not sufficient to distinguish clearly the two signals. In opposition, ore concentrates and slags present a yield much higher than the background with discernible alpha particles emissions at their characteristic energies. Microstructural and elemental analyses by μ-PIXE, μ-RBS and SEM-EDS didn't detect (down to their detection limits) heterogeneities, impurities or any special feature that could have hindered a correct collection of the alpha particles signal in the metallic samples. Nevertheless, TSAC spectra showed that some samples had a superficial contamination by ^{210}Po which was not detected by the other techniques.

From the results presented in this work, there is no evidence of a preferential depletion of ^{226}Ra in a melted metal with respect to the other radionuclides. However, due to the variety of mechanisms operating in a smelting furnace more data are required in order to increase their representativity. With this goal, three archaeometallurgical experiments for tin smelting are ongoing to study ores from different origins and will undergo the same analysis described in this work.

There is also in progress a Monte Carlo simulation of cosmic rays crossing the PIPS detector using the GEANT4 Toolkit [13]. This will give a better understanding of the background signal in the TSAC spectra and the possibilities to decrease it. This is especially important for the analysis of metallic samples.

References

[1] I. Liritzis, Medit. Archaeol. Archaeom 6 (2) (2006) 81–95.
[2] I. Liritzis, A.K. Singhvi, J.K. Feathers, G.A. Wagner, A. Kadereit, N. Zacharias, S.-H. Li, Luminescence Dating in Archaeology, Anthropology and Geoarchaeology: An Overview, SpringerBriefs in Earth System Sciences, 2013.
[3] I. Liritzis, I. Arfara, C. Sideris, Medit. Archaeol. Archaeom. 6 (2) (2006) 93–98.
[4] G. Faure, Principles of isotopic geology, John Wiley & Sons, New York, 1986.
[5] N. Zacharias, E. Kabouroglou, Y. Bassiakos, C.T. Michael, Radiat. Meas. 43 (2008) 791–796.
[6] C.T. Michael, N. Zacharias, A. Hein, Medit. Archaeol. Archaeom 10 (4) (2010) 99–105.
[7] www.canberra.com (Canberra Industries, Inc., Meriden, U.S.A.). Last accessed: 29th of July, 2015.
[8] L.C. Alves, M.B.H. Breese, E. Alves, A. Paúl, M.R. da Silva, M.F. da Silva, J.C. Soares, Nucl. Instrum. Methods B 161–163 (2000) 334–338.
[9] G.W. Grime, M. Dawson, Nucl. Instrum. Methods B 104 (1995) 107–113.
[10] J.A. Maxwell, W.J. Teesdale, J.L. Campbell, Nucl. Instrum. And Methods B 95 (1995) 407.
[11] N.P. Barradas, C. Jeynes, K.P. Homewood, B.J. Sealy, M. Milosavljevic, Nucl. Instrum. Methods B 139 (1998) 235.
[12] http://www.epa.gov/radiation/sources/tobacco.html (U.S. Environmental Protection Agency). Last accessed: 29th of July, 2015.
[13] http://geant4.cern.ch. Last accessed: 29th of July, 2015.